Pulse transient hot strip technique adapted for slab sample geometry to study anisotropic thermal transport properties of μm-thin crystalline films

Y. Ma,[1] J. S. Gustavsson,[2] Å. Haglund,[2] M. Gustavsson,[1,a)] and S. E. Gustafsson[3]
[1]*Hot Disk AB, Chalmers Science Park, SE-41288 Gothenburg, Sweden*
[2]*Photonics Laboratory, Department of Microtechnology and Nanoscience, Chalmers University of Technology, SE-41296, Gothenburg, Sweden*
[3]*Thermetrol AB, Chalmers Science Park, SE-41288 Gothenburg, Sweden*

(Received 18 March 2014; accepted 6 April 2014; published online 25 April 2014)

A new method based on the adaptation of the Pulse Transient Hot Strip technique to slab sample geometry has been developed for studying thermal conductivity and thermal diffusivity of anisotropic thin film materials (<50 μm) with thermal conductivity in the 0.01–100 W/mK range, deposited on thin substrates (i.e., wafers). Strength of this technique is that it provides a well-controlled thermal probing depth, making it possible to probe a predetermined depth of the sample layer and thereby avoiding the influence from material(s) deeper down in the sample. To verify the technique a series of measurements were conducted on a y-cut single crystal quartz wafer. A Hot Strip sensor (32-μm wide, 3.2-mm long) was deposited along two orthogonal crystallographic (x- and z-) directions and two independent pulse transients were recorded. Thereafter, the data was fitted to our theoretical model, and the anisotropic thermal transport properties were determined. Using a thermal probing depth of only 30 μm, we obtained a thermal conductivity along the perpendicular (parallel) direction to the z-, i.e., optic axis of 6.48 (11.4) W/mK, and a thermal diffusivity of 3.62 (6.52) mm^2/s. This yields a volumetric specific heat of 1.79 MJ/mK. These values agree well with tabulated data on bulk crystalline quartz supporting the accuracy of the technique, and the obtained standard deviation of less than 2.7% demonstrates the precision of this new measurement technique. © *2014 Author(s). All article content, except where otherwise noted, is licensed under a Creative Commons Attribution 3.0 Unported License.* [http://dx.doi.org/10.1063/1.4871589]

I. INTRODUCTION

For studying bulk thermal transport properties of solids, transient methods have become increasingly popular and useful since they can handle limited sample sizes (typically 1–10 mm thick), and are insensitive to the thermal contact resistance between the heating/sensing element(s) and the sample surface. The rather simple sample preparation and heat/sensor element fixation to the sample has led to many commercially available instruments based on transient methods.[1–4]

To study samples that are thinner, i.e., thickness $< 100\ \mu$m, and which have relative high thermal conductivity, i.e., $\lambda > 1$ W/mK, a number of transient methods have been developed or specially adapted, including the Pulse Transient Hot Strip (PTHS) method,[5–7] Three-Omega method,[8] and the Thermo-Reflectance method.[9] However, among these only the PTHS method can be used to deduce anisotropic thermal transport properties, from a single transient recording.[10] While for Transient Line Source techniques, like the Three-Omega method, or Transient Point Source techniques, like the Thermo-reflectance method, only one thermal transport property is retrieved. Moreover, Transient Plane Source methods have the advantage of a clearly defined thermal probing depth (as described in Sec. II), making it possible to certify that the measurement results are not influenced by the thermal properties of the material(s)/substrate below the thin layer under investigation.

In the PTHS method a thin micrometer-wide metal strip, a so-called Hot Strip sensor, is deposited on the surface of the sample layer, acting both as the heating and sensing element. While an electrical current, consisting of series of square pulse trains of low duty cycle, passes through the sensor, the average temperature increase in the sensor is monitored via its increased electrical resistance. The recorded average temperature rise as a function of pulse length is thereafter fitted to a theoretical model, wherefrom both the thermal conductivity and thermal diffusivity of the sample layer can be extracted.[11]

In this work we have extended the theory behind the PTHS method so that it does not assume that the thin sample layer is placed on an "infinitely" thick substrate, but instead handles the case where the layer is placed on a thin substrate attached to a heat sink. This technique is referred to as Slab PTHS method and it opens up the possibility to study a wide range of anisotropic material (e.g., crystalline) structures grown on thin wafers (typically 200–600 μm thick). This is of interest, for example, to the semiconductor industry in their continuous efforts to develop/optimize complex layered structures for electronic and photonic devices.

To demonstrate the Slab PTHS technique, the paper is organized as follows: Sec. II contains a discussion on the thermal probing depth; Sec. III outlines the theory; Sec. IV

a)Author to whom correspondence should be addressed. Electronic mail: mattias.gustavsson@hotdiskinstruments.com

 ©Author(s) 2014

This article is copyrighted as indicated in the article. Reuse of AIP content is subject to the terms at: http://scitationnew.aip.org/termsconditions. Downloaded to IP: 219.232.26.91 On: Fri, 07 Aug 2015 00:28:04

describes the measurement setup and procedure; Sec. V summarizes experimental results on single crystal quartz wafer; and Sec. VI rounds up with conclusions and outlook.

II. THERMAL PROBING DEPTH

There are specific requirements on performing thermal transport property measurements using Transient Plane Source techniques, like the Transient Hot Strip[11] and Hot Disc[12] techniques. In particular, it is necessary to use a thin Hot Strip (Hot Disc) sensor, which acts both as heating and sensing element, of a width (disc radius) which closely approximates the desired probing depth, because then the highest accuracy of the retrieved thermal diffusivity and thermal conductivity from the single transient recording is achieved.[13] Further, the heating current through the sensor must consist of close-to-ideal square pulse(s) to make sure that the thermal probing depth matches the strip width (disc radius).

A relevant question is then how deep into the sample the thermal properties are recorded when performing the transient recording. Carslaw and Jaeger[14] discussed the "mean square distribution of heat" while the more useful concept of "probing depth" has recently been introduced[1] and is defined as

$$\Delta_p = k \cdot (\kappa \cdot t)^{1/2}, \tag{1}$$

where k is a constant dependent on the experimental method and the sensitivity by which the temperature increase in the heating/sensing element is recorded, κ is the thermal diffusivity, and t is the length of the square pulse used in the experiment. For Transient Plane Source techniques the constant k is regularly fixed to the value of 2.[1] From this expression it follows that for a given material with a certain thermal diffusivity, the thermal depth of probing into a sample is determined by the current pulse length applied to the heating/sensing element.

From Eq. (1) it is also clear that if the aim is to reduce the probing depth from 10 mm down to 10 μm, i.e., three orders of magnitude, for the same sample material, it is necessary to reduce the current pulse length from the typical range of seconds down to microseconds. A convenient way of working with such short pulses was demonstrated by Gustafsson *et al.*,[5] who used an AC coupled network originally devised by Rosenthal[15] and also used by researchers at Bell Laboratories.[16] This PTHS method has proven successful in handling the electrical aspects of the use of micrometer-wide Hot Strip sensors exposed to trains of microsecond square-shaped current pulses of duty cycle around 5%,[5] and is the basis of this work.

III. SLAB PTHS THEORY

The heating/sensing element is assumed to be a thin rectangular-shaped metal strip deposited on the top surface of a slab-shaped sample, and where the bottom surface of the slab sample is attached to a heat sink, i.e., the sample is placed on a platform that is kept at a constant temperature throughout the transient recording. The thickness of the sample is considered to range from several millimetres down to a fraction of a millimetre.

If the sample is anisotropic and homogeneous, and if the length ($2h$) of the strip is much larger, at least 20 times larger,[11] than the width ($2d$) of the strip, the temperature increase of this element can be expressed as[10]

$$\Delta T(t) = \frac{Q}{2\sqrt{\pi} \cdot h \cdot (\lambda_1 \cdot \lambda_2)^{1/2}} \cdot f(\tau), \tag{2}$$

where Q is the total output of power in the strip and $f(\tau)$ is an analytical function with

$$\tau = (t/\theta_2)^{1/2} \text{ and } \theta_2 = d^2/\kappa_2. \tag{3}$$

Here, t is the time measured from the beginning of the square current or power pulse, which is heating the strip. Parameter λ_1 denotes the thermal conductivity and κ_1 denotes the thermal diffusivity (utilized later in Eq. (11)), both perpendicular to the plane on top of which the strip has been deposited (often referred to as the through-plane direction). Parameters λ_2 and κ_2 are the thermal conductivity and thermal diffusivity, respectively, parallel to the plane on top of which the strip has been deposited (often referred to as the in-plane), but perpendicular to the length of the extended strip.

It is here assumed that the strip is heated by a train of ideal square pulses of low duty cycle (typically 5%) produced by a pulse generator. The electrical circuit used in this AC-coupled network is depicted in Fig. 1, where the AC-coupling is achieved by using a DC block.

The pulse generator, which is assumed to produce time limited ideal square pulses of constant voltage V while having a constant internal resistance R_S, is represented by V and R_S in Fig. 1. The resistance of the Hot Strip sensor can be described by $R(t) = R_0 + \Delta R$, where ΔR is the resistance increase caused by the temperature increase resulting from the direct Joule heating. The resistance, R, of the Hot Strip sensor exposed to a small temperature increase, ΔT, can also be expressed as

$$R = R_0 \cdot [1 + \alpha \cdot \Delta T], \tag{4}$$

where α is the TCR (Temperature Coefficient of the Resistivity), and thus

$$\Delta R = \alpha \cdot R_0 \cdot \Delta T. \tag{5}$$

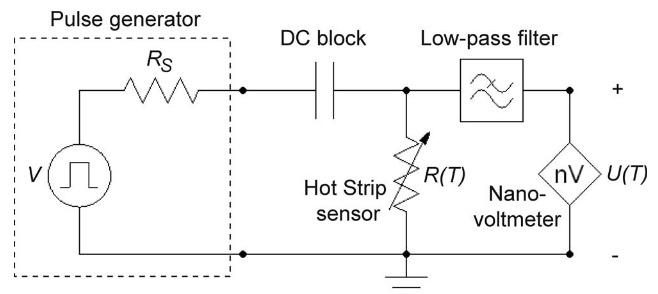

FIG. 1. Electrical circuit for the Slab PTHS method, where the DC block is used to ensure an AC-coupled network, and the low-pass filter is used to facilitate the recording of the time-average voltage increase in the Hot Strip sensor by the nano-voltmeter.

This article is copyrighted as indicated in the article. Reuse of AIP content is subject to the terms at: http://scitationnew.aip.org/termsconditions. Downloaded to IP: 219.232.26.91 On: Fri, 07 Aug 2015 00:28:04

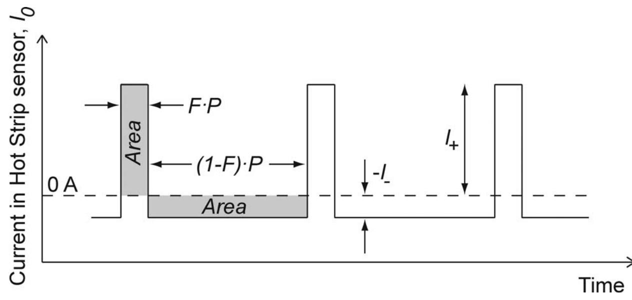

FIG. 2. Train of current pulses passing through the Hot Strip sensor. Note that the zero net-charge condition of the AC-coupled network results in the gray-shaded regions having equal area.

With the notations given in Fig. 1 and the assumption that the pulse voltage V is constant throughout a transient recording, the corresponding voltage over the Hot Strip sensor is $U(t) = U_0 + \Delta U$, where

$$\Delta U = \Delta R \cdot I_0 \cdot \left[\frac{R_S}{R_S + R_0}\right], \tag{6}$$

provided ΔR is small compared with $R_S + R_0$.

The AC-coupled network ideally results in a square-shaped current pulse train through the Hot Strip sensor that is defined by the pulse period P, duty cycle F, and the pulse height, as shown in Fig. 2.

Because of the AC-coupling, the strip is exposed to a series of positive and negative current pulses, of which relative amplitudes are determined by the duty cycle. Let I_+ and I_- be the positive and negative current excursions through the Hot Strip sensor for a fixed duty cycle (F). With the driving voltage (V) and the internal resistance of the pulse generator (R_S), we have

$$V = (R_0 + R_S) \cdot (I_+ - I_-) \tag{7}$$

and

$$I_+ \cdot F = -I_- \cdot (1 - F) \text{ (i.e. zero net charge condition).} \tag{8}$$

The negative or "reverse" current – together with an equivalent part of the current during the positive pulse excursions – create a constant output of power $R_0 \cdot (I_-)^2$, which after a large number of pulses will result in a constant "background" temperature difference (ΔT_b) between the Hot Strip sensor and the temperature controlled platform, on top of which the slab sample has been placed. The thickness of the sample is assumed to be much larger than the thermal probing depth as calculated from the longest pulse length used in the transient recordings. The "background" temperature increase can be expressed as

$$\Delta T_b(t) = \frac{P_0 \cdot F^2}{2\sqrt{\pi} \cdot h \cdot (\lambda_1 \cdot \lambda_2)^{1/2}} \cdot f_S(\tau_{2b}), \tag{9}$$

where P_0 is the total output of power in the strip, and is related to the driving voltage (V) via

$$P_0 = \frac{V^2 \cdot R_0}{(R_0 + R_S)^2}. \tag{10}$$

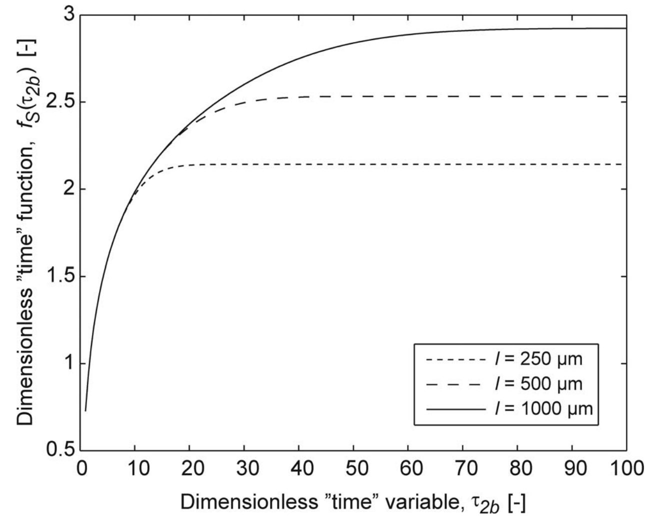

FIG. 3. Time-dependent part of the "background" temperature increase, calculated for different slab sample thicknesses and for a strip width of 32 μm.

Function $f_S(\tau_{2b})$ is a dimensionless time function given by

$$f_S(\tau_{2b}) = \int_0^{\tau_{2b}} dx \cdot \left(1 + 2 \cdot \sum_{n=1}^{\infty} (-1)^n \cdot \exp\left\{-\frac{n^2 \cdot v}{x^2}\right\}\right) \cdot \left(erf\left\{\frac{1}{x}\right\} - \frac{x}{\sqrt{\pi}}\left[1 - \exp\left\{-\frac{1}{x^2}\right\}\right]\right), \tag{11}$$

where $v = \frac{l^2 \cdot \kappa_2}{d^2 \cdot \kappa_1}$, n is an integer, and l is the thickness of the slab sample.

By performing the experiment over a "comparatively" long time, the "background" temperature increase – established by the comparatively small constant output of power $(R_0 \cdot (I_-)^2)$ – will eventually lead to where the function $f_S(\tau_{2b})$ will attain a constant value – as is clear from Fig. 3. This "comparatively" long time is, for example, less than 1 s, if $\tau_{2b} = 100$, the thermal diffusivity κ is 4 mm^2/s, and the strip width is 32 μm. With this assumption we can write down this relatively small "background" temperature increase as follows:

$$\Delta T_b = \frac{P_0 \cdot F^2}{2\sqrt{\pi} \cdot h \cdot (\lambda_1 \cdot \lambda_2)^{1/2}} \cdot \beta, \tag{12}$$

where β here can be considered a constant.

The total temperature increase in the Hot Strip sensor during a pulse is

$$\Delta T_{tot}(t) = \frac{P_0}{2\sqrt{\pi} \cdot h \cdot (\lambda_1 \cdot \lambda_2)^{1/2}} \cdot f(\tau), \tag{13}$$

where

$$f(\tau) = \int_0^{\tau} dx \cdot \left(erf\left\{\frac{1}{x}\right\} - \frac{x}{\sqrt{\pi}}\left[1 - \exp\left\{-\frac{1}{x^2}\right\}\right]\right). \tag{14}$$

When ΔT_b has attained a constant value, we can view the temperature variation during one period as a certain temperature increase during the pulse from the generator (on-state), and as zero temperature increase while the generator is idle (off-state). For small duty cycle, around 5%, the temperature

This article is copyrighted as indicated in the article. Reuse of AIP content is subject to the terms at: http://scitationnew.aip.org/termsconditions. Downloaded to IP: 219.232.26.91 On: Fri, 07 Aug 2015 00:28:04

reached at the end of a pulse "on-state" will have time to relax back to the background temperature, ΔT_b, before the start of the next pulse "on-state.". The time-dependent part of the temperature increase in the Hot Strip sensor during a pulse ($\Delta T(t)$) can then be described as

$$\Delta T(t) = \Delta T_{tot}(t) - \Delta T_b = \frac{P_0}{2\sqrt{\pi} \cdot h \cdot (\lambda_1 \cdot \lambda_2)^{1/2}} \cdot [f(\tau) - F^2 \cdot \beta]. \quad (15)$$

Using Eqs. (5) and (6), the temperature increase $\Delta T(t)$ can be obtained from the voltage increase over the Hot Strip sensor as

$$\Delta T(t) = \Delta U(t) \cdot \frac{(R_0 + R_S)^2}{\alpha \cdot V \cdot R_0 \cdot R_S}, \quad (16)$$

where the relationship $I_0 = V/(R_0 + R_S)$ has been used. (17)

By measuring the average voltage over a large number of periods, it is possible to get the average temperature increase over a full pulse period or over a pulse "on-state". In the AC network, this is done with the nano-voltmeter with assistance of the low-pass filter. The average temperature increase in the Hot Strip sensor, ΔT_{MV}, over a full pulse period is

$$\Delta T_{MV}(P) = \frac{P_0}{2\sqrt{\pi} \cdot h \cdot (\lambda_1 \cdot \lambda_2)^{1/2}} \cdot \frac{1}{P} \cdot \int_0^{FP} dt \cdot [f(\tau) - F^2 \cdot \beta]. \quad (18)$$

It is here assumed that the temperature variation, above the "background" temperature during the part of the period when the pulse generator is idle, is obscured by the fact that the total "reverse" current is used to maintain the "background" temperature. The corresponding average temperature increase over a pulse "on-state" can then be expressed as

$$\Delta T_{MV}(FP) = T_+ \cdot \frac{1}{FP} \cdot \int_0^{FP} dt \cdot [f(\tau) - F^2 \cdot \beta], \quad (19)$$

where

$$T_+ = \frac{P_0}{2\sqrt{\pi} \cdot h \cdot (\lambda_1 \cdot \lambda_2)^{1/2}}. \quad (20)$$

Equation (19) can be expressed as

$$\Delta T_{MV}(\tau_2) = T_+ \cdot \left(\frac{2}{\tau_2^2} \cdot \int_0^{\tau_2} dx \cdot x \cdot f(x) - \beta \cdot F^2 \right), \quad (21)$$

using the transformation

$$\tau_2 = \left(\frac{FP}{\theta_2} \right)^{1/2}, \text{ where } \theta_2 = \frac{d^2}{\kappa_2}. \quad (22)$$

Equation (21) can be transformed to

$$\Delta T_{MV}(\tau_2) = T_+ \cdot H(\tau_2) - \beta \cdot T_+ \cdot F^2 \quad (23)$$

with

$$H(\tau_2) = \frac{2}{\tau_2^2} \cdot \left(\int_0^{\tau_2} dx \cdot x \cdot f(x) \right). \quad (24)$$

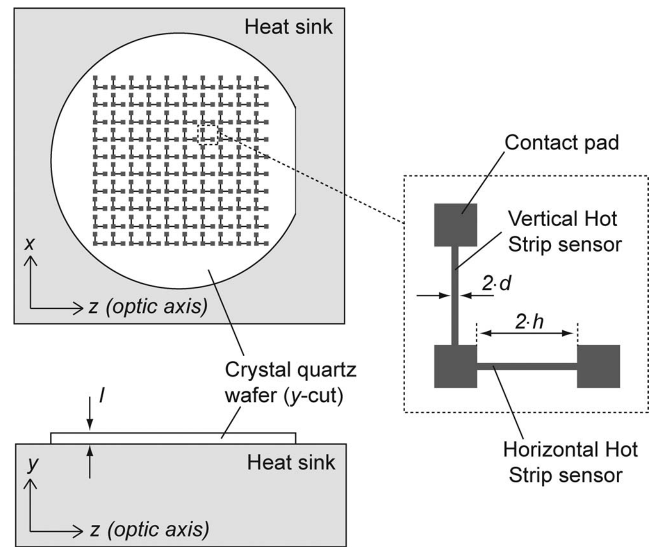

FIG. 4. Schematic top (above) and side (bottom) view of the heat sink platform with the quartz wafer placed on top, also illustrating the Hot Strip sensor layout and orientation with respect to the crystallographic axes of the wafer.

From Eq. (23) it can be seen that a plot of measured $\Delta T_{MV}(\tau_2)$ (the mean value of the temperature increase in the Hot Strip sensor over a pulse "on-state") versus calculated $H(\tau_2)$ would give a straight line fit with slope T_+. Since the thermal diffusivity κ_2 is not known, an iteration process is initiated to find the θ_2-value that gives the best straight line fit between measured $\Delta T_{MV}(\tau_2)$ and calculated $H(\tau_2)$, using the least square method. From the θ_2-value, which gives the best straight line fit, the "in plane" thermal diffusivity can be calculated from

$$\kappa_2 = \frac{d^2}{\theta_2}. \quad (25)$$

From the slope of the straight line, T_+, the product of the two thermal conductivities can be calculated:

$$(\lambda_1 \cdot \lambda_2)^{1/2} = \frac{P_0}{2\sqrt{\pi} \cdot h \cdot T_+}. \quad (26)$$

If the specific heat per unit volume, ρC_p, is measured in a separate experiment, it is possible to calculate the two conductivities and the two diffusivities in the principal directions. These directions should correspond to the orientations of the Hot Strip sensor, see Fig. 4. However, if the anisotropic sample is a uniaxial crystal – like single crystal quartz – and the Hot Strip sensor is oriented along the optic- (z-) axis, the measurement yields the thermal conductivity and the thermal diffusivity in the plane perpendicular to the optic-axis, and from their ratio the volumetric specific heat for the sample can be obtained, which is demonstrated below.

IV. MEASUREMENT SETUP AND PROCEDURE

A y-cut surface-polished single crystal quartz wafer (z-cut flat) from MTI Corporation, with diameter 2 in. and thickness 500 μm, was measured to verify the Slab PTHS method. The aim is to demonstrate the unique ability of the method to determine the anisotropic thermal conductivity and thermal diffusivity of a crystalline sample, only requiring a thermal

This article is copyrighted as indicated in the article. Reuse of AIP content is subject to the terms at: http://scitationnew.aip.org/termsconditions. Downloaded to IP: 219.232.26.91 On: Fri, 07 Aug 2015 00:28:04

probing depth of less than 50 μm, which expands the capability to study μm-thin crystalline films.

Figure 4 shows a schematic of the Hot Strip sensor layout on the single crystal quartz wafer. A matrix of a double Hot Strip sensor pattern was distributed evenly on the surface of the y-cut quartz wafer. The double strip pattern was arranged such that one strip was oriented along the optic- (z-) axis (referred to as horizontal strip), and the other strip was oriented along the x-axis (referred to as vertical strip), of the crystal. A thermal probing depth of about 30 μm was the target wherefore the strips were 32-μm wide (in order to maximize the sensitivity in the dual determination of the thermal conductivity and diffusivity from a single pulse transient recording, as discussed in Sec. II). To further ensure that systematic errors in the measured thermal transport properties are less than 1%, the strip length was 100 times longer than the strip width, i.e., 3.2 mm. The strips were fabricated by electron beam evaporation of 10 nm Ti ("adhesive" layer) and 97 nm Au, followed by a subsequent lift-off step. This yielded a strip resistance (R_0) of ~32 Ω (which is not too far from a desired 50 Ω for impedance matching to the internal resistance of the pulse generator, $R_S = 50$ Ω). The quartz wafer was placed on an aluminium heat sink platform with precise temperature control by a Peltier element and a TEC controller. For ensuring good thermal contact between the wafer and the platform, a thin layer of thermal paste was used.

Electrical connections to the Hot Strip sensors were arranged with contact pads at the ends of the strips that were probed using micro-manipulated probe positioners (having a ball tip needle that can handle high DC currents) with the aid of a microscope. In the applied electrical circuit (Fig. 1) the DC block is designed such that AC-coupling is achieved, but without deforming the square-shaped pulses reaching the Hot Strip sensor, which requires a relative large capacitance. During the pulse transient recording, the voltage over the Hot Strip sensor varies quite substantially, especially as the applied pulse voltage is in the range 1–10 V. For this reason it was necessary to use a specially designed low-pass filter to comply with the performance of the nano-voltmeter, when recording the average voltage increase of the Hot Strip sensor. The particular instrumentation used for these measurements, as well as software for controlling the experiment and analysing the recorded data, was developed by Hot Disk AB.[17]

The measurements were conducted by first measuring the TCR value of the Hot Strip sensor, by scanning the heat sink platform temperature over a range of 20 °C around room temperature (22 °C) and simultaneously recording the change in sensor resistance. The TCR was ~0.0032 Ω/K, and also constant after exposing the Hot Strip sensors to a series of pulse transient recordings. Next, the heat sink platform temperature was stabilized at 22 °C, and a series of pulse trains of fixed voltage and duty cycle (5%), but of different pulse lengths, were applied to the Hot Strip sensor. The average voltage increase of the sensor for each pulse length was recorded by the nano-voltmeter. The average voltage increase is proportional to the average temperature increase of the Hot Strip sensor (ΔT_{MV}), which is plotted in Fig. 5 versus pulse length ($F \cdot P$). The pulse length was varied between 4 and 70 μs, where the longest pulse length yields a maximum temperature increase of ~1 K.

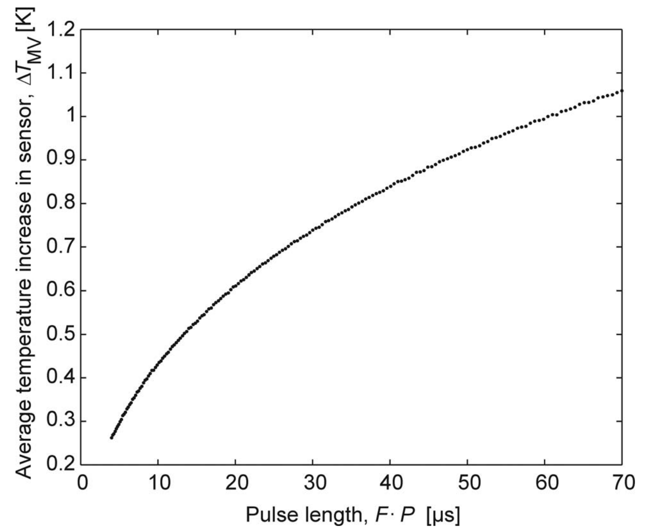

FIG. 5. Measured average temperature increase over a pulse "on state" in a horizontal 32-μm-wide Hot Strip sensor as a function of pulse length, for a fixed set pulse voltage of 2 V and a duty cycle of 5%.

It should be noted that when recording the average voltage increase in the Hot Strip sensor for a particular pulse length, a certain number of "prior" pulse periods are required in the pulse train to ensure that the condition of having a constant "background" temperature, ΔT_b, as expressed by Eqs. (9) and (12), is fulfilled, see also Fig. 3. Therefore, for the case in Fig. 5, with a 500-μm-thick single crystal quartz wafer, the number of "prior" pulse periods in a pulse train had to be around 100-200 periods, or more.

From the recorded average temperature increase of the Hot Strip sensor (ΔT_{MV}) versus pulse length, the thermal transport properties are calculated via an iteration procedure as described in Sec. III, seeking the best straight line fit of a

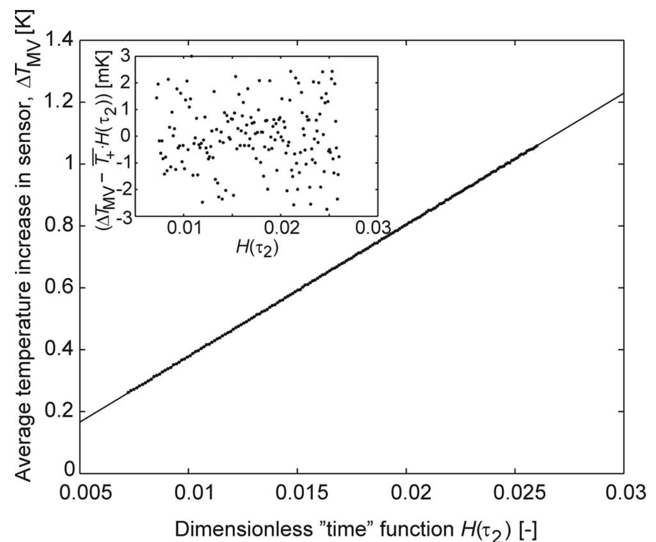

FIG. 6. Best straight line fit of calculated dimensionless "time" function H(τ_2) to measured average temperature increase ΔT_{MV} in a 32-μm-wide horizontal Hot Strip sensor for different pulse lengths. The inset shows the deviation of measured ΔT_{MV} from the straight line, resulting in a standard deviation of 1.3 mK.

This article is copyrighted as indicated in the article. Reuse of AIP content is subject to the terms at: http://scitationnew.aip.org/termsconditions. Downloaded to IP: 219.232.26.91 On: Fri, 07 Aug 2015 00:28:04

TABLE I. Measured thermal conductivity and thermal diffusivity in direction perpendicular to the optic-axis of y-cut single crystal quartz wafer, using the Slab PTHS method with a thermal probing depth of 30 μm.

Horizontal Strip No.	TCR (ΩK^{-1})	Set pulse voltage ($V/2$) (V)	Output of Power (P_0) (mW)	ΔT (K)	$\lambda_\perp$ ($Wm^{-1}K^{-1}$)	$\kappa_\perp$ (mm^2s^{-1})	ρC_p ($MJm^{-1}K^{-1}$)
1	0.00320	1.7	55.1	0.750	6.512	3.616	1.801
		2	76.2	1.046	6.438	3.482	1.849
		2.3	100.8	1.390	6.457	3.513	1.838
2	0.00323	1.7	55.2	0.728	6.682	3.761	1.776
		2	76.4	1.051	6.539	3.632	1.801
		2.3	101.0	1.397	6.562	3.636	1.805
3	0.00319	1.7	55.4	0.760	6.392	3.720	1.718
		2	76.6	1.063	6.383	3.638	1.755
		2.3	101.3	1.405	6.379	3.579	1.782
	Mean Value				6.483	3.620	1.792
	Std Dev%				1.56%	2.45%	2.24%

calculated dimensionless "time" function $H(\tau_2)$ to measured ΔT_{MV} for different pulse lengths. For the particular measurement data presented in Fig. 5, the obtained best straight line fit is shown in Fig. 6, where the standard deviation of the measurement data to the straight line is only 1.3 mK.

V. EXPERIMENTAL RESULTS

A series of pulse transient recordings at different pulse voltages were conducted on three different horizontal, and three different vertical, Hot Strip sensors. The measurement conditions and results when using the horizontal strips are summarized in Table I. For each pulse voltage, two individual recordings were made and the average values from these two recordings are tabulated. Since the horizontal strip is oriented along the optic- (z-) axis, the extracted thermal diffusivity is for x-direction (see Fig. 4, and Eq. (25)) and the extracted thermal conductivity product (see Eq. (26)) is for x-y-direction. But because of single crystal quartz being a uniaxial crystal, the material properties along the principal x- and y-axis are identical, and therefore the results directly yield the thermal conductivity ($\lambda_\perp$) and thermal diffusivity ($\kappa_\perp$) perpendicular to the optic-axis. In addition, from their ratio we can determine the volumetric specific heat of the single crystal quartz, which would not be possible if the sample was a biaxial crystal. To limit the thermal probing depth to $\sim$30 μm (i.e., close to the width of the strip) a maximum pulse length of 70 μs was used, and to achieve a temperature increases of $\sim$1 K over this pulse length, an instrument set pulse voltage ($V\,/\,2$ referring to Fig. 1) around 2 V was needed. A temperature increase of 1-2 K is typically required when working with TPS techniques to avoid impairments from Johnson noise. Moreover, as can be observed in Table I, no deterministic change of the extracted thermal transport properties was found when varying the instrument set pulse voltage around 2 V, which supports the theory behind the method.

Table II summarizes the corresponding measurement conditions and results when using the vertical strips. In this case the strip is oriented along the x-axis, wherefore the extracted thermal diffusivity is for z-direction and the extracted thermal conductivity product is for z-y-direction. This means that we obtain the thermal diffusivity parallel to the optic-axis ($\kappa_\parallel$), and the geometric mean value of the thermal conductivity parallel and perpendicular to the optic axis ($\sqrt{\lambda_\perp \lambda_\parallel}$). Because of the higher thermal diffusivity and thermal conductivity in these directions, a shorter maximum pulse length

TABLE II. Measured thermal conductivity and thermal diffusivity in direction parallel to the optic-axis of y-cut single crystal quartz wafer, using the Slab PTHS method with a thermal probing depth of 34 μm.

Vertical Strip No.	TCR (ΩK^{-1})	Set pulse voltage ($V/2$) (V)	Output of Power (P_0) (mW)	ΔT (K)	$\sqrt{(\lambda_\perp \lambda_\parallel)}$ ($W \cdot m^{-1}K^{-1}$)	$\kappa_\parallel$ (mm^2s^{-1})
4	0.00323	2	76.0	0.859	8.488	6.201
		2.25	96.2	1.091	8.584	6.464
		2.5	118.8	1.348	8.627	6.537
5	0.00327	2	76.4	0.869	8.744	6.505
		2.25	96.6	1.103	8.696	6.494
		2.5	119.3	1.365	8.704	6.443
6	0.00322	2	76.1	0.847	8.607	6.750
		2.25	96.4	1.111	8.567	6.787
		2.5	119.0	1.375	8.492	6.534
	Mean Value				8.612	6.524
	Std Dev%				1.05%	2.63%

This article is copyrighted as indicated in the article. Reuse of AIP content is subject to the terms at: http://scitationnew.aip.org/termsconditions. Downloaded to IP: 219.232.26.91 On: Fri, 07 Aug 2015 00:28:04

TABLE III. Summary of measured anisotropic thermal transport properties of y-cut single crystal quartz wafer, using the Slab PTHS method with a thermal probing depth of ~30 μm.

	$\lambda_{\perp}$ ($W \cdot m^{-1}K^{-1}$)	$\kappa_{\perp}$ (mm^2s^{-1})	$\lambda_{\parallel}$ ($W \cdot m^{-1}K^{-1}$)	$\kappa_{\parallel}$ (mm^2s^{-1})	ρC_p ($MJ \cdot m^{-1}K^{-1}$)
Mean Value	6.483	3.620	11.442	6.524	1.792
Std Dev%	1.56%	2.45%	1.45%	2.63%	2.24%

of 50 μs and a somewhat higher pulse voltage was used to reach a ~30 μm thermal probing depth and to achieve ~1 K temperature increase.

Table III summarizes the measured anisotropic thermal transport properties of the y-cut single crystal quartz wafer, using a thermal probing depth of only ~30 μm. The results are taken as the mean values from all data presented in Tables I and II. In order to obtain the thermal conductivity in the direction parallel to the optic axis ($\lambda_{\parallel}$), the values of the thermal conductivity from both Tables I and II were used. The obtained experimental data with the Slab PTHS method are quite close to earlier published data on anisotropic thermal transport properties of bulk single crystal quartz, see, e.g., Refs.11, 18, and 19. The results also imply that the y-cut wafer under test does not display any structural defects within the investigated probing depth (~30 μm), since thermal transport properties are sensitive to even slight deviations from an ideal crystalline structure. Further, the low standard deviation in the obtained thermal transport properties, <2.7% for all properties, demonstrates the high precision of the Slab PTHS technique.

VI. CONCLUSIONS

In this paper, we have presented a new measurement technique, referred to as Slab PTHS method, for analyzing anisotropic thermal transport properties of the top part of a wafer material, by probing a region between the top surface down to a depth of <50 μm. To verify the technique, i.e., investigate the accuracy and precision, a series of measurements were performed on a 500-μm-thick y-cut single crystal quartz wafer. By using a pulse transient recording with square-shaped pulses of maximum length 70 μs and duty cycle 5%, the thermal probing depth was limited to ~30 μm. The acquired average temperature increase in the Hot Strip sensor versus pulse length was fitted to a theoretical model that assumes a slab sample of "finite" thickness, and positioned on an "ideal" heat sink. From these fittings, the thermal conductivity and thermal diffusivity tensors, and volumetric specific heat, of single crystal quartz could be determined with a precision better than 2.7%, and the obtained average values agree well to literature values on the corresponding bulk properties.

As a remark, the Slab PTHS method does not exclude the possibility of measuring the anisotropic thermal transport properties of a crystalline thin film (<50 μm) deposited on a substrate of different material, which is of high practical importance in, e.g., the semiconductor industry. The conditions for obtaining the "true" thermal transport properties of the thin film are (a) to use a thermal probing depth of the transient recording that does not exceed the thickness of the thin film, and (b) to ensure that a constant "background" temperature (ΔT_b) between the Hot Strip sensor and the heat sink (i.e., the bottom side of the substrate) has been established, by using a certain minimum number of pulse periods in the applied pulse trains. To overestimate the number of periods, one could, for example, calculate $f_S(\tau_{2b})$ assuming the sample (i.e., substrate with thin film) has a thermal conductivity which is the lowest of the (estimated) values for the substrate or thin film. Finally, it should be noted that the thin film may also consist of a multilayered material stack, in which case the measured properties would be the effective thermal transport properties over the thermal probing depth.

ACKNOWLEDGMENTS

The authors wish to thank Professor Klas Yhland and Dr. Jörgen Stenarsson, SP Technical Research Institute of Sweden, for their assistance in designing the AC-coupled network. This work has been financially supported by the Area of Advance Nanoscience and Nanotechnology, Chalmers University of Technology, Sweden.

[1]International standard: ISO 22007-2 (2008).
[2]International standard: ISO 22007-3 (2008).
[3]International standard: ISO 22007-4 (2008).
[4]International standard: ISO 8894-1 (2010).
[5]S. E. Gustafsson, M. A. Chohan, K. Ahmed, and A. Maqsood, J. Appl. Phys. **55**(9), 3348 (1984).
[6]M. Gustavsson, H. Nagai, and T. Okutani, Rev. Sci. Instrum. **74**, 4542 (2003).
[7]M. Gustavsson, H. Nagai, and T. Okutani, Int. J. Thermophys. **26**(6), 1803 (2005).
[8]D. G. Cahill and R. O. Pohl, Phys. Rev. B **35**, 4067 (1987).
[9]D. G. Cahill, W. K. Ford, K. E. Goodson, G. D. Mahan, A. Majumdar, H. J. Maris, R. Merlin, and S. R. Phillpot, J. Appl. Phys. **93**(2), 793 (2003).
[10]S. E. Gustafsson, E. Karawacki, and M. N. Khan, J. Appl. Phys. **52**(4), 2596 (1981).
[11]S. E. Gustafsson, E. Karawacki, and M. N. Khan, J. Phys. D: Appl. Phys. **12**, 1411 (1979).
[12]S. E. Gustafsson, Rev. Sci. Instrum. **62**(3), 797 (1991).
[13]V. Bohac, M. K. Gustavsson, L. Kubicar, and S. E. Gustafsson, Rev. Sci. Instrum. **71**(6), 2452 (2000).
[14]H. S. Carslaw and J. C. Jaeger, *Conduction of Heat in Solids*, 2nd ed. (Oxford University Press, 1971).
[15]L. A. Rosenthal, Rev. Sci. Instrum. **43**(11), 1575 (1972).
[16]A. T. English, G. L. Miller, D. A. H. Robinson, L. V. Dodd, and T. Chynoweth, J. Appl. Phys. **49**(2), 717 (1978).
[17]See www.hotdiskinstruments.com for company information on Hot Disk AB.
[18]C. Clauser and E. Huenges, Thermal conductivity of rocks and minerals, AGU Reference Shelf (1995).
[19]E. H. Ratcliffe, Br. J. Appl. Phys. **10**, 22 (1959).

This article is copyrighted as indicated in the article. Reuse of AIP content is subject to the terms at: http://scitationnew.aip.org/termsconditions. Downloaded to IP: 219.232.26.91 On: Fri, 07 Aug 2015 00:28:04